Hindawi Publishing Corporation
Journal of Coatings
Volume 2013, Article ID 613178, 7 pages
http://dx.doi.org/10.1155/2013/613178

Research Article

Friction and Wear Properties of Cold Gas Dynamic Sprayed α-Al_2O_3-Al Composite Coatings

Jie Wu, Yongshan Tao, Huazi Jin, Ming Li, Tianying Xiong, and Chao Sun

State Key Laboratory of Corrosion and Protection, Institute of Metal Research, CAS, Shengyang 110016, China

Correspondence should be addressed to Yongshan Tao; ystao@imr.ac.cn

Received 21 March 2013; Revised 11 June 2013; Accepted 30 June 2013

Academic Editor: Wenya Li

Different proportions of α-Al_2O_3 and pure Al powders were coated onto AZ91D magnesium alloy substrates by cold gas dynamic spray. The microstructure and morphologies of the coatings were observed by scanning electron microscope. The friction and wear properties were tested by a ball-on-disk wear tester. It was found that the interfaces between grains and substrates formed close boundaries. It is revealed that the composite coatings could increase the friction or wear properties of the coatings. It was observed that the wear of coatings was converted from adhesive wear into abrasive wear with α-Al_2O_3 particles increasing and that the adhesive wear accompanied with abrasive wear would increase the wear rate of coatings.

1. Introduction

The electroless plating and plating process will seriously cause detrimental effects to the environment and the human health. Therefore, research for alternatives of electroless plating and plating has been widely carried out in the world [1, 2]. Cold gas dynamic sprayed (CGDS) metal and cermet coatings are adopted increasingly in industry as an alternative for electroless plating and plating since such coating technique can provide a superb friction and wear resistance.

CGDS, as a new technique for the surface coating fabrication, has been developed rapidly in recent years and attracted more and more scientists' interests. In CGDS process, microparticles are accelerated to supersonic velocities and impact onto a substrate surface; the coating is formed by plastic deformation of sprayed particles in a solid state during impact in cold spraying. In this technique process, the sprayed particles at speed over 500–1200 m/s [3–12] and at gas temperatures up to around 300–900 K can be deposited onto a wide range of substrate materials. The temperature of sprayed particles prior to impact is much lower than their melting point, and then spray materials experience little microstructure change, oxidation, or decomposition. Figure 1 shows the schematic drawing of CGDS system.

In this paper, α-Al_2O_3 and Al powders were sprayed onto the surface of magnesium alloy by CGDS. The microstructure and morphology of the coating, friction, and wear properties were studied; the phase and structures of the coating were also researched.

2. Experiments

2.1. Experimental Materials and Instruments. As-cast AZ91D magnesium alloy, the most widely used material up to now, was applied as substrates which were cut into 25 mm in diameter and 5 mm in depth. All the substrates were ground with SiC paper down to grit 800 and ultrasonically cleaned using acetone. Commercially pure aluminum powder (99.5 wt.%) produced by gas atomization was blended with α-Al_2O_3 particles produced by electric furnace melting down as feedstock materials for coatings [13–15]. As seen in Figure 2 and Table 1, the spherical pure Al particles and the irregular lath-like α-Al_2O_3 particles were in the average size of 25 μm. The corresponding weight percentages of α-Al_2O_3 in the feedstock were 25%, 50%, and 75%, and the coatings prepared from these composite powders were denoted as coating25, coating50, and coating75, respectively. The mixture powders

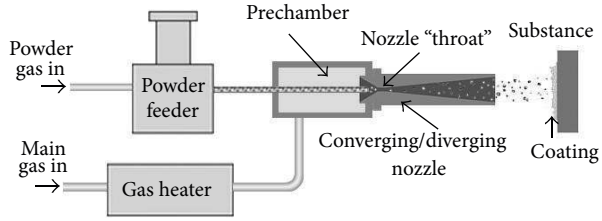

Figure 1: Schematic illustration of CGDS.

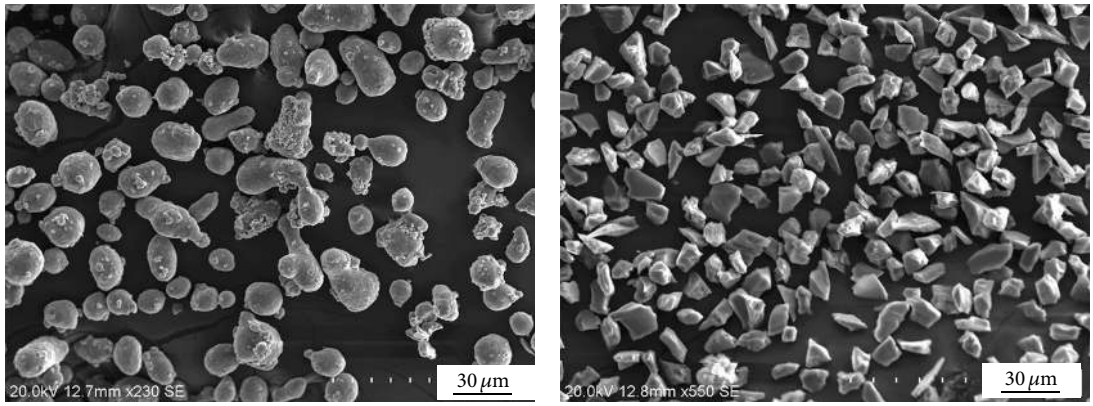

(a) (b)

Figure 2: SEM images of as-received feedstock powders of (a) pure Al and (b) α-Al_2O_3.

Table 1: Volume distribution of particles with different diameter.

	Volume distribution %			
	<10 μm	10–20 μm	20–30 μm	>30 μm
Al	7	31	40	22
α-Al_2O_3	10	29	37	24

Table 2: Key spraying parameters.

Gas pressure (MPa)	Gas temperature (°C)	Spray distance (mm)	Feeder voltage (mV)
1.6 ± 0.1	230 ± 5	30	28

in different proportions were mixed for 8 hours in the high-efficient flip mixer. The most crucial determinations of gas pressure, gas temperature, spray distance, and feeder voltage of spraying parameters were listed in Table 2.

The friction and wear properties of coatings were evaluated by using a ball-on-disk wear tester (Figure 3). Coated disk surfaces were polished by diamond grinding and finished by buffing. The ball material was chosen GCr15 of 6.35mm as conveyor rolls that could bond the running substrates. After ultrasonically cleaning the pin and washing the disk in acetone, they were fixed to the test apparatus. The diameter of contact trail was 23.78 mm. In this experiment, the revolving speed was ensured at 30 r/min for the entire test, and the load between the pin and the disk was 10 N. The abrasiveness of coatings was measured after 5 min ball milling, and the wear volume was recorded by surface profilometer Micro XAM-3D during the wear test.

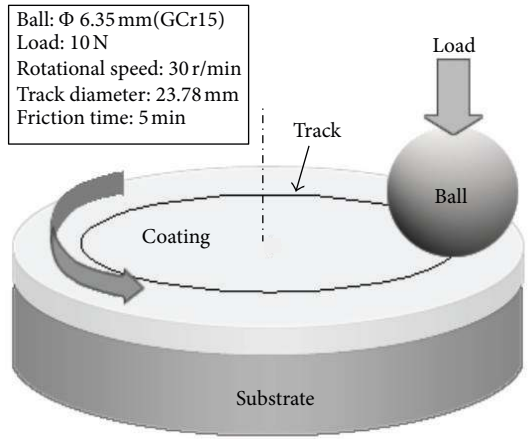

Figure 3: Picture of ball-on-disk friction pair.

2.2. Morphologies of Coatings. The abrasiveness on the cross-section of coatings was measured by a ball-on-disk wear tester at a load of 10 N. The cross-section of coatings produced by suitable techniques of grinding, polishing, and etching was observed by scanning electron microscope (SEM). Figure 4 shows the morphologies of the coating-substrate interface of pure Al coating, coating25 and coating50, and reveals that coating50 was bonded with matrix more tightly than pure

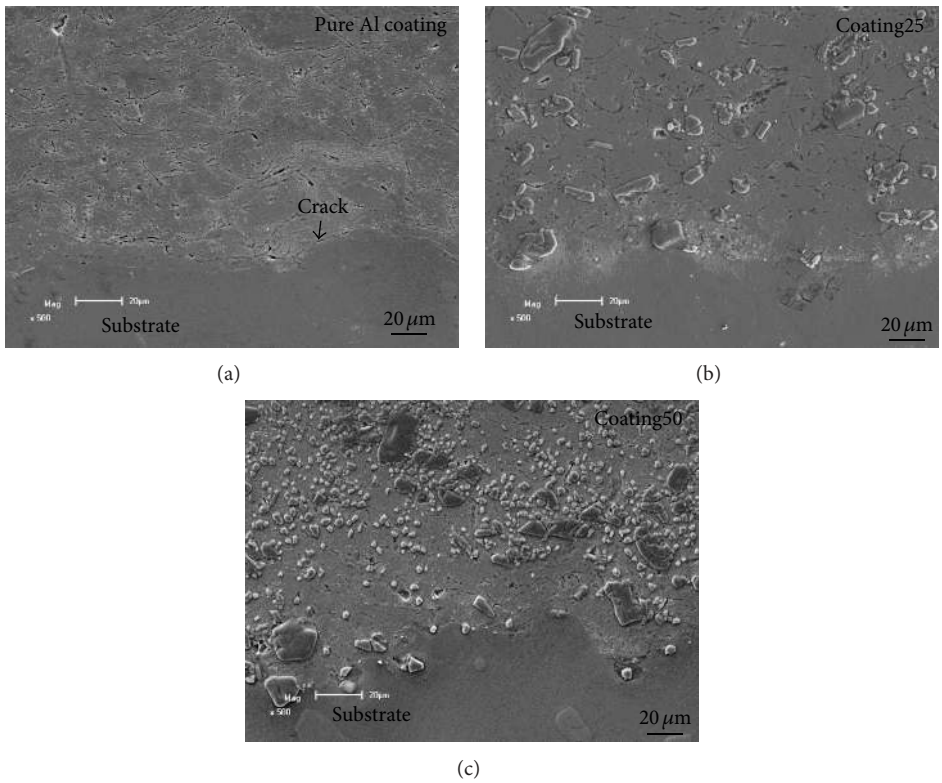

FIGURE 4: Etched cross-section morphologies of (a) pure Al coating, (b) coating25, and (c) coating50 showing the coating-substrate interface.

Al and coating25, and parts of alumina particles were deeply embedded into the matrix as well. It has been studied and found out by the experiment that the low deposition on the matrix to the point where α-Al_2O_3 particles were easily and completely detached from the matrix to decrease the boundary defection of coating-matrix interface have been played a role of bonding strength, while the embedded α-Al_2O_3 particles which produced a "serration" bonding between the coatings and the matrix were another contributing factor.

The morphologies of the section of coatings in three cold spray conditions Figures 5(a)–5(c) and the surface of coatings Figures 5(d)–5(f) were observed by SEM shown in Figure 5. The obviously comparable information was detailed in Table 3. It has been found that the amount of porosities on the surface of these composite coatings Figures 5(d)–5(f) was attributed to vacancies by detached alumina particles in the process of polishing and burnishing, while the section of coatings Figures 5(a)–5(c) did not see the detaching. The characteristic structure of cold sprayed coatings may be the contributing factor. If the surface is considered as a vertical plant of spraying, the intensively deformed aluminum particles as dish-like aggregated together may cause the small size of α-Al_2O_3 particles to be embedded between the upper and lower aluminum particles along the spraying direction. The process of polishing and burnishing on the surface caused the small sized of alumina particles to be detached easily from the matrix under the shear forces, while the same approach on the section caused them to be detached difficultly from the opposite direction of the embedded particles and shear force.

3. Results and Discussion

3.1. Peening Effect. In the course of cold sprayed coating, the deposited metal particles were impacted on the surface accompanying plastic deformation. In the former study, it has been known that the coarsening of alumina in a certain range was prior to impacting on the surface with a high velocity of transition; the subsequent one in a low deformability and a high hardness grew a larger deformation. As far as cold sprayed coating concerned, in order to obtain the dense structure of coatings, the most important factor is fully complete deformation. In Figures 5(e) and 5(f), it is obviously shown that the size of alumina particles deposited in these composite coatings were generally smaller than the pure Al coating. Compared with the feedstock powder, the sizes of alumina particle of coating25, coating50 and coating75 should be selected according to the statistics from our experiments, because such sizes can control the diameter of the particles within the range of 22 μm to 12 μm; it was a more extensive range than that of the mixed powder. It may be explained by following factors: (a) the in-flight alumina particles break into small-size particles during impacting each other resulted in the small particles being increased; (b) the small alumina particles obtained at the higher velocity resulted in the small particles being more easily deposited in coatings than the large ones.

3.2. Different Proportion Coatings on the Friction and Wear Properties. Figure 6 shows wear volume per unit wear time

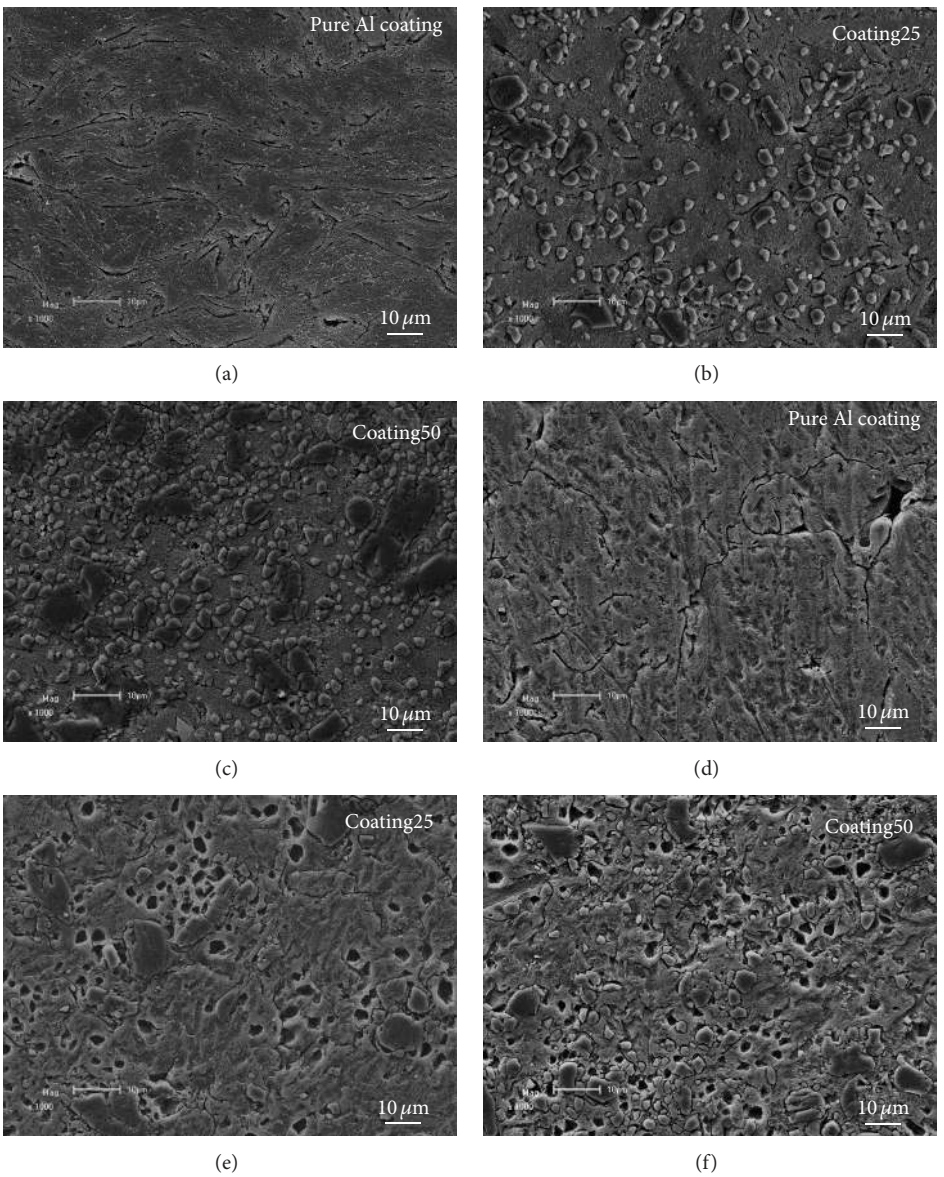

Figure 5: SEM observation of the lightly etched cross-sectional samples of (a), (b), and (c) and surface samples of (d), (e), and (f) for pure Al coating, coating25, and coating50, respectively.

Table 3: Porosity of the coatings produced by cold spraying.

Coating type	Pure Al coating	Coating25	Coating50
Porosity (%)	1.53	0.55	0.30

of the coatings. As compared to the continuously rising microhardness under the certain spraying conditions recommended, there was no correlation between increased content of alumina and coatings wear effectiveness. The wear rate of coating25 was slightly higher than the pure Al coating, the wear rate of coating50 significantly increased more than Coating25 by one times, but Coating75 greatly decreased.

The friction and wear properties were analyzed with the wear rate accompanying the morphology of grinding crack. In accordance with the experiment, it was found that coating50s grinding crack was wide and deep but coating75s was shallow and narrow; the pure Al's grinding crack had a large and thin metal sheet which adheres to the coatings and protrudes above the coatings and extends the grinding crack to become a higher embossing than the standard plane and a large beaded shiny-white edge. It is considered that the beaded edge may cause not only the uncontinuous grinding crack but also the more extensive negative deviation when calculating the wear volume. In the interior of these composite coatings, a large sheet adhered or the extensive embossing produced by protrusion and extension was not found.

Figure 7 shows the morphology of wear track in different wear mode observed by SEM. Pure Al showed the smearing of

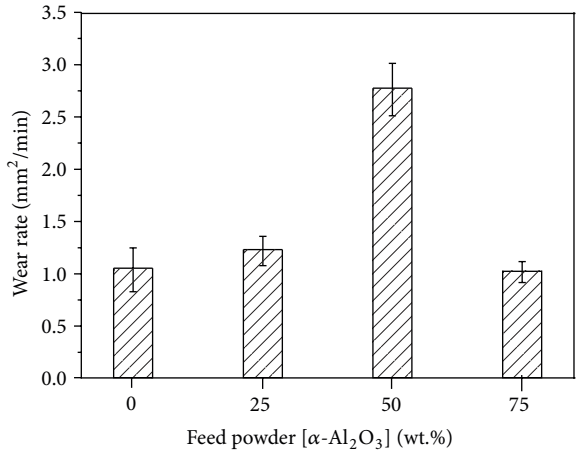

Figure 6: Wear volume per unit wear time of the coatings.

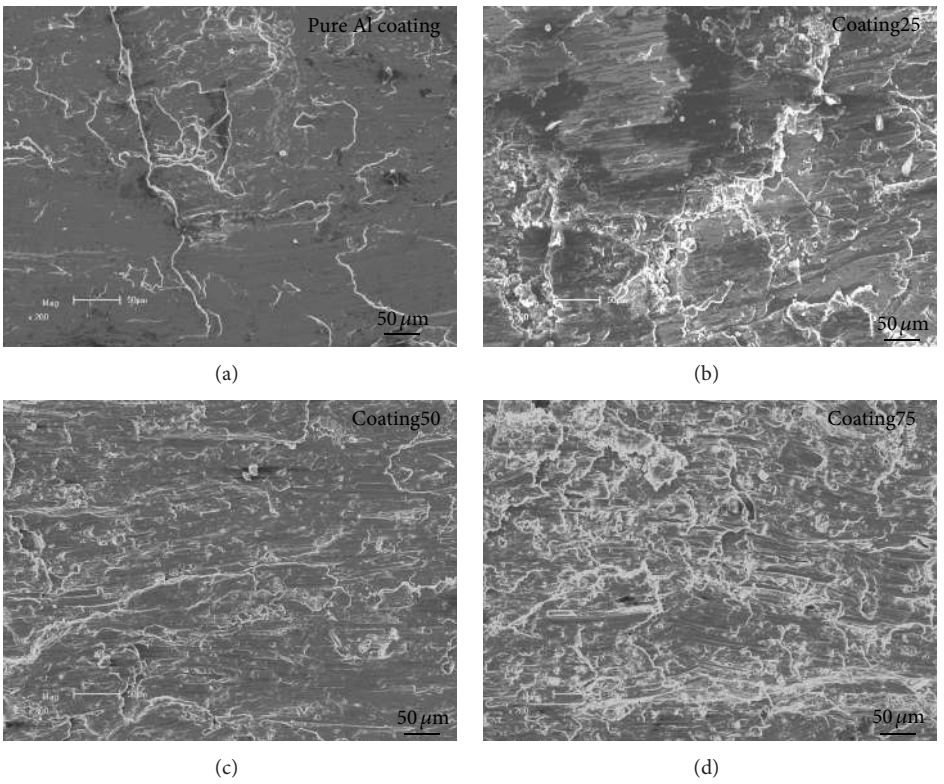

Figure 7: SEM of the wear track showing different wear mode between (a) the pure Al coating and (b–d) the composite coatings.

the wear track, combined with the extrusion and embossing analyzed previous, which was considered as the typically adhesive wear. In addition, as compared with the aluminum debris that adhered to the surface of friction-pair steel ball during the ball milling in the wear test, the transition into adhesive wear in the process of dry friction was also explained and the regularity about "matter translocation" that the high-strength surface adheres to the soft material in the course of adhesive wear was illustrated as well. Coating25 and coating50 gave the similar morphology of smearing as that of pure Al coating, but there were some ploughing and small-scale wear debris. It was observed that coating50's ploughing was denser and more obvious, and the abrasive wear occurred between the two coatings accompanying the adhesive wear. With the more obvious and denser ploughing, wear debris could be observed in coating75 but the smearing of wear trace was hard to find. It was regarded that the wear mode of Coating75 was a complete transition into abrasive wear. As a conclusion from the analyzed previous, the increased α-Al_2O_3 particles may cause the wear mode to be transformed

from the adhesive wear to abrasive wear. Therefore, according to the wear rate in the variation as a-Al2O3 particles increased, the wear rate increases first and subsequently decreases, of the first increased after reduced increased α-Al_2O_3 particles, it can be inferred and explained that the adhesive wear and abrasive wear occurred collaboratively and synchronously may increase the wear rate of coating, however may reduce however if not that may reduce the wear rate on the contrary on the contrary.

3.3. Friction Coefficient and Sliding Wear Time on the Friction and Wear Properties. The variation of the friction coefficient as another contributing factor of the friction and wear properties was assessed. The variation of friction coefficient of these coatings with the wear time was plotted in Figure 8. It was indicated that Al coating, coating25, and coating50 showed a higher variation of friction coefficient in the beginning of the friction except for coating75, in which it was considered that the related adhesive wear could explain the transition from the soft coating material to hard-steel ball and the fragmentation in the continuous grinding crack as the extensive embossing. In the experiment it was also found that the use of the friction pair in same material may decrease the absolute friction coefficient and the amplitude of the friction coefficient.

3.4. Friction and Wear Properties Analysis. It was researched by this experiment that α-Al_2O_3 supplied to the rubbing surfaces during milling influences the severe-mild wear transition via analyzing the microstructure and morphologies. The α-Al_2O_3 particles were found to play an important role in mechanism of wear; the wear type of coating was changed from adhesive wear into abrasive wear by increasing the content of the supplied particles. It is generally accepted that the oxide content in cold sprayed coatings will tend to increase by decreasing the size of spray powder if the spray powder size decreases, since smaller particles are oxidized more due to the high specific surface area and the tendency that smaller particles are heated to high velocity during spraying as the high-specific surface area and a high velocity during the spraying, also the smaller particles are more oxidized. Coating can be formed even on hard substrate when the contents and size of hard particles in the incident stream of spray are large enough. Therefore, the particle shape could have an influence on coating's properties, such as the craters generated by the impact of hard particles at the interface between composite coatings and substrate. To select raw materials for this type of cold spray, final fragmented size and shape of particles should be counted. If such oxides are finely dispersed in the coatings, cold sprayed coatings have a potential to generate small oxide wear debris autogenously.

As the number of Al_2O_3 particles were increased in the coating, more fragmented Al_2O_3 particles from the initial particles were observed among the Al particles. And it was also observed that only very fine Al_2O_3 particles were embedded in the Al matrix. That relatively soft Al substrate was damaged to form craters by attacking the fragmented Al2O3 particles fragmented Al_2O_3 particles. To confirm the correlation between adhesion wear and abrasive wear of coatings at the interface, the wear volumes were measured in Figure 6 and the wear time were measured in Figure 8. As mentioned previous, such craters in Al powders by cold spray process were not generated at the interface. For this reason, the adhesion of pure Al coatings was the lowest among the coatings. However, Al-α-Al_2O_3 coating with the ratio of 1 : 1 wt% has the highest value of wear. It is very possible that the large and big craters could be generated between the coatings and substrate. Al-α-Al_2O_3 composites using different metal/ceramic compositions and particle morphologies were successfully coated on Al substrates through using the cold spray process. There are good possibilities that cold spray coating of hard materials incorporated with pure Al can be successfully performed.

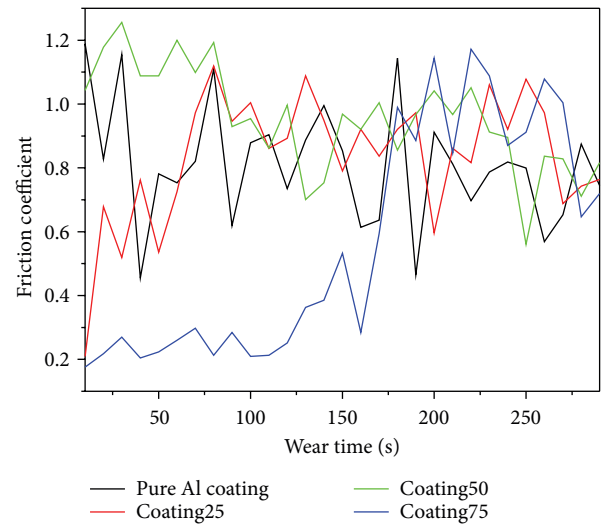

Figure 8: Friction coefficient versus wear time for the coatings.

4. Conclusions

(1) The bonding strength of the composite coatings is higher than that of pure Al coating because of α-Al_2O_3 particles cleaning and pinning effect.

(2) At a load of 10 N, the mixed α-Al_2O_3 particles are not indicated to improve the wear resistance, and the wear of coatings was converted from adhesive wear into abrasive wear with α-Al_2O_3 particles being increased.

(3) The possibility of metallurgical bonding between Al/Al particles interface increases because α-Al_2O_3 particles enhance the deformation of Al particles and the tensile strength of composite coatings is much higher than that of pure aluminum coatings because α-Al_2O_3 particles inhibit the crack extension.

References

[1] B. Sartwell, K. Legg, and J. Sauer, "Validation of WC/Co HVOF thermal spray coatings as a replacement for hard chrome plating

on aircraft landing gear, part I: material testing," Joint Test Report, U.S. Department of Defense, 2002.

[2] J. G. Legoux, B. Arsenault, L. Leblanc, V. Bouyer, and C. Moreau, "Evaluation of four high velocity thermal spray guns using WC-10% CO-4% Cr cermets," *Journal of Thermal Spray Technology*, vol. 11, no. 1, pp. 86–94, 2002.

[3] R. C. McCune, W. T. Donlon, O. O. Popoola, and E. L. Cartwright, "Characterization of copper layers produced by cold gas-dynamic spraying," *Journal of Thermal Spray Technology*, vol. 9, no. 1, pp. 73–82, 2000.

[4] K. Sakaki and Y. Shimizu, "Effect of the increase in the entrance convergent section length of the gun nozzle on the high-velocity oxygen fuel and cold spray process," *Journal of Thermal Spray Technology*, vol. 10, no. 3, pp. 487–496, 2001.

[5] R. C. Dykhuizen and M. F. Smith, "Gas dynamic principles of cold spray," *Journal of Thermal Spray Technology*, vol. 7, no. 2, pp. 205–212, 1998.

[6] R. C. Dykhuizen, M. F. Smith, D. L. Gilmore, R. A. Neiser, X. Jiang, and S. Sampath, "Impact of high velocity cold spray particles," *Journal of Thermal Spray Technology*, vol. 8, no. 4, pp. 559–564, 1999.

[7] T. H. van Steenkiste, "Kinetic spray: a new coating process," *Key Engineering Materials*, vol. 197, pp. 59–85, 2001.

[8] T. H. van Steenkiste, J. R. Smith, and R. E. Teets, "Aluminum coatings via kinetic spray with relatively large powder particles," *Surface and Coatings Technology*, vol. 154, no. 2-3, pp. 237–252, 2002.

[9] D. L. Gilmore, R. C. Dykhuizen, R. A. Neiser, T. J. Roemer, and M. F. Smith, "Particle velocity and deposition efficiency in the cold spray process," *Journal of Thermal Spray Technology*, vol. 8, no. 4, pp. 576–582, 1999.

[10] R. S. Lima, J. Karthikeyan, C. M. Kay, J. Lindemann, and C. C. Berndt, "Microstructural characteristics of cold-sprayed nanostructured WC-Co coatings," *Thin Solid Films*, vol. 416, no. 1-2, pp. 129–135, 2002.

[11] H. Y. Lee, Y. H. Yu, Y. C. Lee, Y. P. Hong, and K. H. Ko, "Cold spray of SiC and Al_2O_3 with soft metal incorporation: a technical contribution," *Journal of Thermal Spray Technology*, vol. 13, no. 2, pp. 184–189, 2004.

[12] A. P. Alkhimov, S. V. Klinkov, V. F. Kosarev, and A. N. Papyrin, "Gas-dynamic spraying. Study of a plane supersonic two-phase jet," *Journal of Applied Mechanics and Technical Physics*, vol. 38, no. 2, pp. 324–330, 1997.

[13] H. Y. Lee, S. H. Jung, S. Y. Lee, Y. H. You, and K. H. Ko, "Correlation between Al_2O_3 particles and interface of Al-Al_2O_3 coatings by cold spray," *Applied Surface Science*, vol. 252, no. 5, pp. 1891–1898, 2005.

[14] Y. Tao, T. Xiong, C. Sun, H. Jin, H. Du, and T. Li, "Effect of α-Al_2O_3 on the properties of cold sprayed Al/α-Al_2O_3 composite coatings on AZ91D magnesium alloy," *Applied Surface Science*, vol. 256, no. 1, pp. 261–266, 2009.

[15] Y. Tao, T. Xiong, C. Sun et al., "Microstructure and corrosion performance of a cold sprayed aluminium coating on AZ91D magnesium alloy," *Corrosion Science*, vol. 52, no. 10, pp. 3191–3197, 2010.